

---

# Quasicrystals

Uwe Grimm<sup>1</sup> and Peter Kramer<sup>2</sup>

<sup>1</sup> Department of Mathematics, The Open University, Walton Hall, Milton Keynes MK7 6AA, UK. Email: [u.g.grimm@open.ac.uk](mailto:u.g.grimm@open.ac.uk)

<sup>2</sup> Institut für Theoretische Physik, Universität Tübingen, 72076 Tübingen, Germany. Email: [peter.kramer@uni-tuebingen.de](mailto:peter.kramer@uni-tuebingen.de)

**Summary.** Mathematicians have been interested in non-periodic tilings of space for decades; however, it was the unexpected discovery of non-periodically ordered structures in intermetallic alloys which brought this subject into the limelight. These fascinating materials, now called quasicrystals, are characterised by the coexistence of long-range atomic order and ‘forbidden’ symmetries which are incompatible with periodic arrangements in three-dimensional space. In the first part of this review, we summarise the main properties of quasicrystals, and describe how their structures relate to non-periodic tilings of space. The celebrated Penrose and Ammann-Beenker tilings are introduced as illustrative examples. The second part provides a closer look at the underlying mathematics. Starting from Bohr’s theory of quasiperiodic functions, a general framework for constructing non-periodic tilings of space is described, and an alternative description as quasiperiodic coverings by overlapping clusters is discussed.

## 1 Aperiodicity and order

In mathematics, interest in non-periodic tilings of space arose in the 1960s, in the context of the decidability of the question whether a given finite set of prototiles admits a tiling of the plane [6]. Some twenty years later, the unexpected discovery of aperiodically ordered crystals in intermetallic alloys [25] brought the subject to the attention of crystallographers, physicists and materials scientists. The existence of quasicrystals raises fundamental questions about the concept of order in nature, and inspired the ongoing investigation of the associated mathematical structures.

### 1.1 Quasicrystals

Crystals are a paradigm of order in nature. Their symmetry, perfection and beauty reflects a perfectly ordered structure at the atomic level. Essentially, the structure of a conventional crystal is based on a single building block, the unit cell, which usually contains a small number of atoms, and the entire

crystal is then made up by periodic repetition of the same building block. For example, in a salt crystal, the unit cell can be chosen to have cubic shape containing an equal number of sodium and chlorine atoms, thus giving rise to a structure with cubic symmetry which is reflected in the morphology of salt crystals.

Crystalline structures have been classified according to their symmetries; we shall discuss the corresponding crystallographic point groups in more detail below. For crystals that are built by periodic repetition of a single building block, hence are based on a three-dimensional lattice, the possible symmetries are limited by the *crystallographic restriction*. Only certain rotational symmetries are compatible with a periodic arrangement in three dimensional space; in particular, such crystals can only have rotational symmetry axes of order 1, 2, 3, 4 and 6. Fivefold or eightfold symmetry, for instance, are crystallographically ‘forbidden’, and are not found in conventional crystals. In particular, this includes *icosahedral symmetry*, which is the symmetry of the icosahedron and the dodecahedron, two Platonic solids shown in Fig. 1.

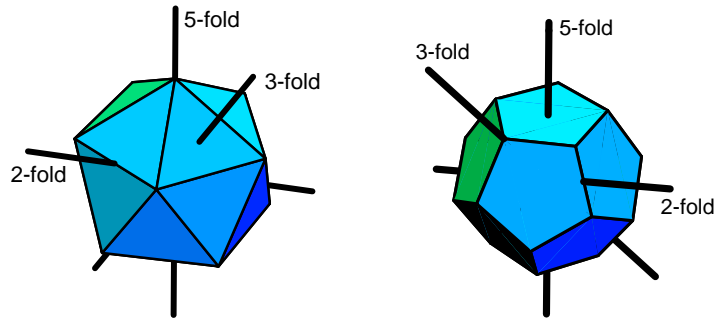


**Fig. 1.** The icosahedron (left) and dodecahedron (right). Symmetry axes of order two, three and five are indicated. There are 15 axes of order 2 (half the number of edges in both cases), 10 axes of order 3 (half the number of faces in the icosahedron or vertices in the dodecahedron) and 6 axes of order 5 (half the number of vertices in the icosahedron or faces in the dodecahedron).

It thus came as a surprise when in 1982 electron diffraction patterns of a rapidly cooled aluminium manganese alloy showed a clear account of icosahedral symmetry [25], which includes ‘forbidden’ five-fold symmetry directions, see Fig. 2 (note that an  $n$ -fold symmetric crystal, with odd  $n$ , produces a  $2n$ -fold symmetric diffraction image). Almost simultaneously, twelve-fold rotational symmetry was observed in a nickel chromium alloy [14]. These materials have the property that their diffraction patterns consist of well defined sharp spots, similar as observed for conventional crystals, which indicates a long-range order of the atomic positions. Due to this structural similarity to conventional crystals, these new solids were called *quasicrystals*. The distinc-

tive property of quasicrystals is their crystallographically forbidden symmetry, which can be observed in diffraction experiments. Such symmetries cannot be accommodated in a periodic lattice structure in three space dimensions, and hence quasicrystals cannot be described by a periodic structure in space based on the repetition of a single unit cell. This means that one is forced to give up the requirement of periodicity, and indeed *aperiodic* tilings of space can account for the observed symmetries, as will be discussed below.

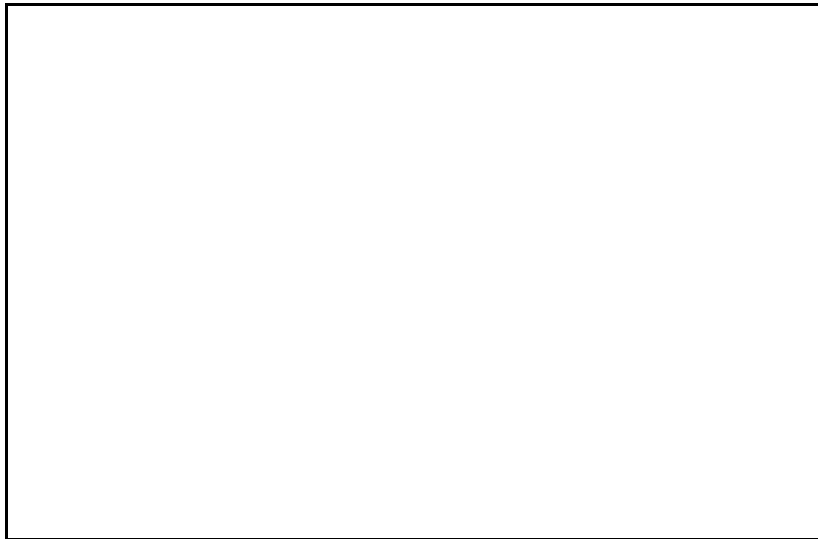


**Fig. 2.** The first published evidence of icosahedral crystals is this selected area electron diffraction pattern obtained by Dan Shechtman [25] from a rapidly cooled aluminium manganese alloy. Angles are measured with respect to a fivefold axis, and the observed 2-, 6- and 10-fold symmetries in the diffraction patterns match the orientation of 2-, 3- and 5-fold axes of icosahedral symmetry, compare Fig. 1. Reprinted figure with permission from D. Shechtman, I. Blech, D. Gratias, J.W. Cahn, *Phys. Rev. Lett.* **53**, 1951 (1984). Copyright (1984) by the American Physical Society.

The two examples mentioned above correspond to two different types of quasicrystals. The diffraction pattern for the aluminium manganese quasicrystal found by Shechtman in 1982 displays icosahedral symmetry; such quasicrystals are known as *icosahedral quasicrystals*. The arrangement of atoms in these quasicrystals is not periodic in any direction of space. In contrast to this, the nickel chromium quasicrystals discovered by Ishimasa and Nissen have a single direction of twelve-fold symmetry, and show periodicity along this twelve-fold symmetry direction. Such systems are called *dodecagonal quasicrystals*, and you can think of them as consisting of layers in which atoms are arranged in a non-periodic, twelve-fold symmetric fashion, which are then stacked periodically in space. Subsequently, such layered quasicrystals have

also been found with ten-fold (*decagonal quasicrystals*) [5] and eight-fold (*octagonal quasicrystals*) [28] symmetry. Over the past twenty years, many other alloy compositions have been shown to give rise to quasicrystals, in particular icosahedral and decagonal phases, but no further symmetries have been found as yet.

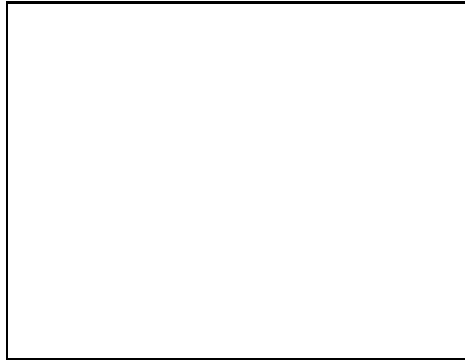


**Fig. 3.** A holmium magnesium zinc ‘single’ quasicrystal [10]. It shows perfect dodecahedral morphology, compare Fig. 1. The background shows a millimetre scale. Reprinted figure with permission from I.R. Fisher, K.O. Cheon, A.F. Panchula, P.C. Canfield, M. Chernikov, H.R. Ott, K. Dennis, *Phys. Rev. B* **59**, 308 (1999). Copyright (1999) by the American Physical Society.

As for a conventional crystal, the symmetry of the atomic arrangement in a quasicrystal often manifests itself in the morphology of high-quality specimens. Detailed and laborious investigations of phase diagrams of ternary alloy systems has made it possible to grow ‘single’ quasicrystals from the melt, providing well characterised samples for experimental studies. An example of a dodecahedral crystal of an holmium magnesium zinc quasicrystal is shown in Fig. 3, showing beautiful facets that perfectly reflect the intrinsic icosahedral order of the alloy. As a consequence of their peculiar atomic arrangements, quasicrystals show interesting physical properties, leading to a number of promising practical applications, in particular as low-friction surface coatings and as storage material for hydrogen.

The aperiodic tilings discussed below offer a simple model structure than can explain the observed symmetries in quasicrystals, and serve as appropriate mathematical idealisations of the atomic structure, in analogy to the role of lattices in conventional crystallography. In nature, there is no truly perfect crystal (even the most expensive diamond contains some defects), and in the same sense the structure of a real quasicrystal will differ considerably from these idealised tilings. In particular, many quasicrystals are high-temperature phases, which hints at the importance of entropy for the stability of these phases, in which case you would expect an inherently disordered structure.

Like many other questions concerning quasicrystals, this is subject of current research activity and scientific debate, and has not yet been satisfactorily understood; see also [15, 24] and [26, 27] for introductory monographs and collections of introductory articles on the mathematics and physics of quasicrystals, and [22, 4, 20] for more in-depth mathematical results.

## 1.2 Crystallographic restriction

Before discussing examples of such tilings, we briefly explain the *crystallographic restriction* mentioned above. It states that in a periodic lattice in two or three dimensions, the only possible non-trivial rotation symmetries are 2-, 3-, 4- and 6-fold symmetry. It is easy to come up with examples of periodic structures that have these symmetries, see Fig. 4. How can one see that other symmetries, such as fivefold symmetry, cannot occur?

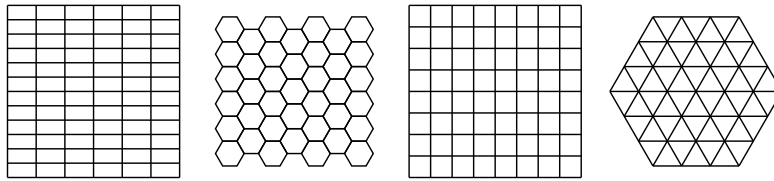


**Fig. 4.** Planar periodic tilings with 2-, 3-, 4- and 6-fold rotational symmetry.

A simple argument goes as follows. Assume for a moment that you had a periodic lattice with fivefold symmetry. This means that you can rotate the lattice by multiples of  $72^\circ$  about any of its lattice points, and obtain the same lattice again. We shall now show that this is impossible.

Start with two lattice points which have minimal distance from each other. Then, we can rotate one point about the other by multiples of  $72^\circ$ , and the four new points obtained in this way must be lattice points as well. Analogously, we can rotate choosing the other point as a centre, which gives us another four new lattice points, see Fig. 5. But now you see that there are lattice points that are closer to each other than the ones we started from, which were supposed to have minimal distance – so we end up with a contradiction, which means that there is no such structure.

If you use the same argument for 2-, 3-, 4- and 6-fold symmetry, no problem arises. Fig. 6 shows (on the left) the case of sixfold symmetry, where rotated latticed points coincide to form an equilateral triangle, which can be extended to a triangular lattice shown in Fig. 4 on the right. For any  $n$ -fold rotational symmetry with  $n > 6$ , this will not happen, and you always obtain two lattice points that are closer than the points you started with, see the right part of Fig. 6 for an example with  $n = 8$ .

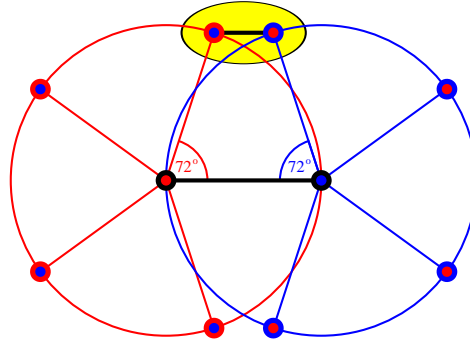


**Fig. 5.** Two starting points (dark), and the two sets of 4 points obtained by rotating one about the other by multiples of  $72^\circ$ . The highlighted pair of rotated points is closer than the pair of rotation centres, leading to the contradiction.

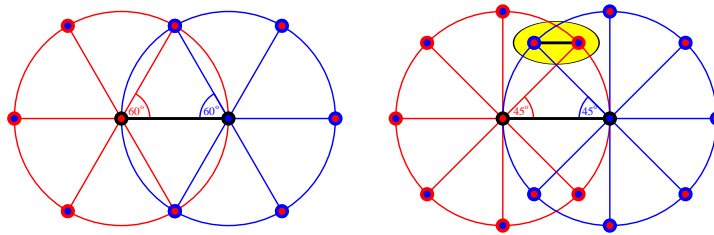


**Fig. 6.** The same as Fig. 5 for the 6-fold (left) and 8-fold (right) case. For the 6-fold case, the points obtained by rotation form part of a triangular lattice, whereas the 8-fold case again leads to a contradiction. Obviously, the same happens for any rotation angle  $360^\circ/n$  with  $n > 6$ , since the corresponding highlighted pair of rotated points is always closer together than the two original points.

No new possibilities arise in three dimensions; however, this is not true for dimensions larger than three. In particular, periodic lattices with 5-, 8- and 12-fold symmetry exist in four dimensions, and in six dimensions you find lattices with full icosahedral symmetry.

### 1.3 Aperiodic tilings

To overcome the limitations imposed by the crystallographic restriction, we have to look at more general classes of tilings, without lattice periodicity. As discussed below, aperiodically ordered tilings can be constructed that reproduce the symmetry seen in diffraction experiments. Paradigmatic examples of such structures are the *Penrose tiling* [23] and the *Ammann-Beenker tiling* [1]. In the following, we briefly introduce these tilings and explain how they can be constructed, while heuristically motivating some of their properties along the way; see also [2] for a gentle introduction, and [12] for the computer

generation of the tilings shown below. A deeper description of the underlying mathematics is given in Sect. 2.

We mention three rather different approaches – matching rules, inflation and projection from higher-dimensional periodic lattices. While the usual examples can be described in any of these settings, they are by no means equivalent. For instance, there are many non-periodic tilings that can be obtained by inflation, but cannot be embedded in a periodic lattice in a finite-dimensional space. Arguably the most powerful approach is the projection method; for example, it can be shown in a rather general setting that such point sets are pure point diffractive, which means that they give rise to point-like diffraction patterns such as shown in Fig. 2.

### Matching rules

Seemingly the simplest way to specify an aperiodic tiling, such as the Penrose tiling, is by so-called *matching rules*. In essence, these are specific rules that restrict the possible local arrangements of the basic tiles. In the simplest examples, matching rules can be encoded by markings (or *decorations*) on, for instance, the edges of the tiles. An example is the rhombic Penrose pattern, which is obtained from two rhombic prototiles with single and double arrows on the edges, as shown in Fig. 7.

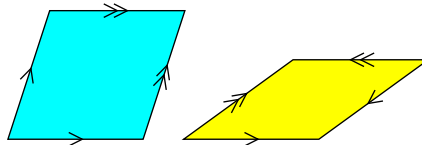


**Fig. 7.** The tiles of the rhombic Penrose tiling with arrow decorations.

Clearly, ignoring the arrows these tiles can give rise to periodic tilings of the plane – as an example just take the tiling made by repeating one of the two tiles periodically. To obtain the Penrose tiling, tiles are assembled subject to the constraint that tiles in the tiling are edge-to-edge and such that the arrow decorations on adjacent edges match. These matching rules ‘enforce’ aperiodicity. A ‘legal’ patch is shown in Fig. 8.

Note that the matching rules do *not* amount to an algorithm that allows you to grow a Penrose tiling. Indeed, it is more like a jigsaw puzzle – if you start putting tiles together you may arrive at a situation where neither of the tiles fits at a particular place, in which case the patch you have grown does not occur in a perfect Penrose tiling. However, if you manage to grow a tiling that fills the plane it is indeed ‘the’ Penrose tiling [23] (or more precisely, a member of the class of *locally indistinguishable* Penrose tilings). In the application to quasicrystals, where it is tempting to associate matching

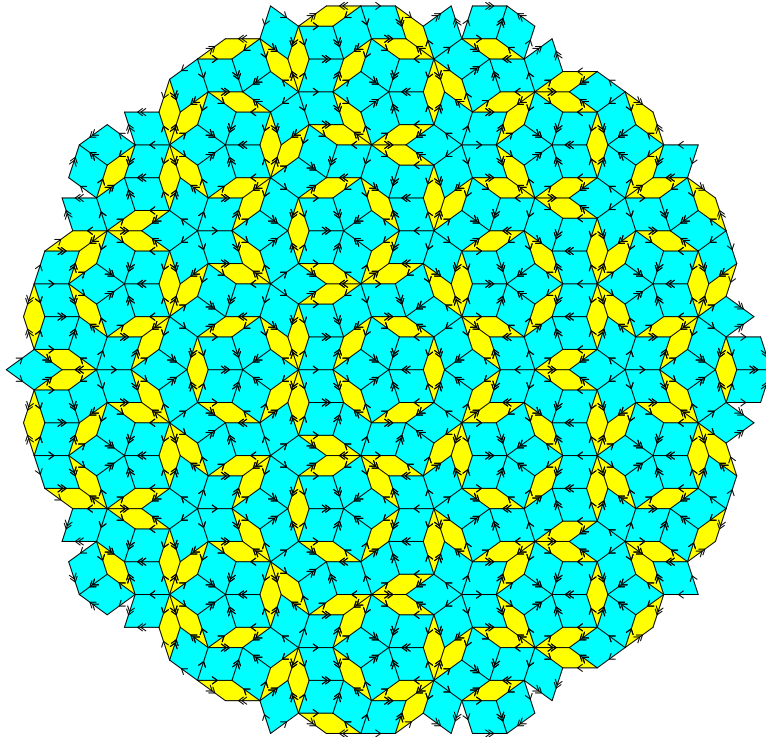


**Fig. 8.** A legal patch of a Penrose tiling.

rules to preferred local arrangement of atoms, this has sparked discussions about how quasicrystals grow, a topic that is still not completely understood, see [11] for a review.

The Ammann-Beenker tiling, again built from two different tiles, has eight-fold rotational symmetry. It also possesses matching rules; however, in this case decorations on edges and vertices are needed to exclude periodic tilings. A legal patch of the tiling, including the matching rules, is shown in Fig. 9.

### Inflation

An important concept for the construction of aperiodically ordered structures is the so-called inflation (or deflation) procedure. It is based on a transformation of the tiles which consists of two steps – the re-scaling by a constant factor (*inflation factor*) and the dissection of the tiles into a number of copies of the original tiles, of the original size. An inflation rule for the Ammann-Beenker tiling is shown in Fig. 10, where for simplicity we use a triangle (half a square) as the basic tile. For this case, the inflation factor is  $1 + \sqrt{2}$ . Note that the



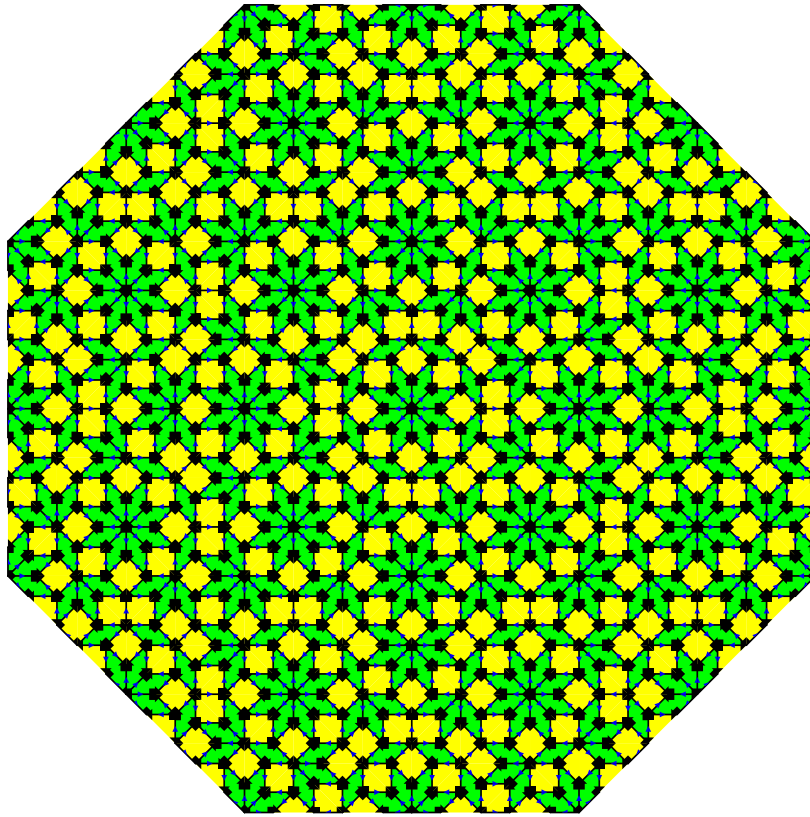


**Fig. 9.** A legal patch of an Ammann-Beenker tiling.

dissection of the triangle breaks the reflection symmetry of the unmarked tiles – you need to consider the orientation of the triangle, marked by the arrow on the hypotenuse. The dissection of a triangle of the opposite orientation is the mirror image of the one shown here.

Now, you can build an Ammann-Beenker tiling by repeated application of this rule, starting for instance from a single tile. After one step, you obtain one of the patches shown at the bottom of Fig. 10. Applying the procedure again, you obtain a patch consisting of more tiles, and so on and so forth. In this way, you can create an arbitrarily large tiling, and the infinite structure obtained in the limit has the property that it is invariant under the inflation procedure. In fact, the octagonal patch of the Ammann-Beenker tiling depicted in Fig. 9 was obtained precisely in this way, by applying inflation starting with an eightfold symmetric patch.

The inflation symmetry of an infinite Ammann-Beenker tiling has an interesting consequence. If you cut out any finite patch from the tiling, then

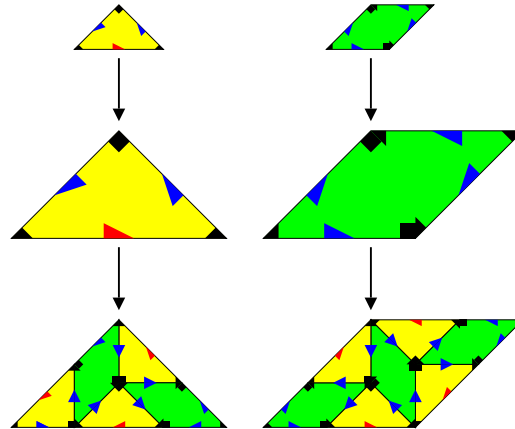


**Fig. 10.** Inflation of the Ammann-Beenker tiling.

this patch will occur in the infinite tiling over and over again. This property is called *repetitivity* (not to be confused with periodicity). You can deduce this property by applying the inverse transformation, *deflation*, to the tiling with your chosen patch. Eventually, after a finite number of steps, your patch will be mapped to a single tile. Since the two tiles occur with positive frequency in the tiling (which can be calculated from the inflation rule), it follows by applying the same number of inflation steps again that the chosen patch also occurs with positive frequency.

In this sense, the Ammann-Beenker tiling is very regular indeed – like in a periodic structure any finite patch repeats in a rather regular fashion, albeit not periodically. So if you find the same feature repeated at a certain distance, it will not necessarily repeat at twice the distance – it may repeat earlier or later, but it will repeat.

### Cut and project sets

The third, and final method discussed in this section, is based on periodic lattices, but in a higher-dimensional space. Let us consider a simple example first. Imagine looking at a huge stack of sugar cubes, all nicely arranged in a regular fashion to form a cubic structure in three dimensions. If you take a horizontal surface (so your pile is a big cube made up of lots of small cubes), and look at it from some angle, you will see a pattern consisting of rhombs, as shown in Fig. 11 on the left. If you look at an inclined surface at commensurate angles, such as shown in the centre of Fig. 11, you find periodic patterns made up of three different rhombs, which are the projections of the faces of cubes, and their shape depends on the inclination of the surface. If you look at a more general surface, you still find a tiling made up of the same three rhombs. However, the rhombic pattern you observe will, except

for special choices of surface, not be periodic. An example is shown on the right of Fig. 11. Even if the surface is ‘flat’, as it is in this case, in general you end up with a non-periodic pattern, such as shown on the right of Fig. 11.

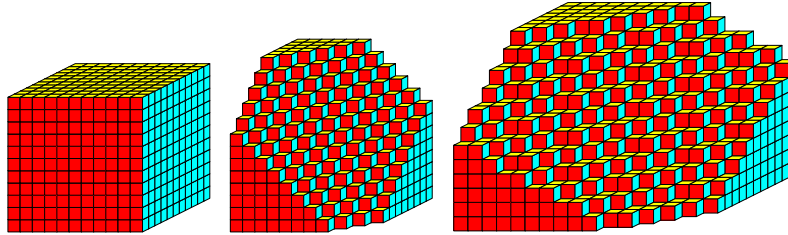


**Fig. 11.** Planar projections of a packing of cubes, showing different surfaces. The projected planar tiling consist of three rhombic tiles, corresponding to the projections of the three visible faces of the cube. Onlye for special surfaces, such as shown on the left and in the centre, the rhombs form a periodic tiling; in general, the rhombic pattern on a surface is non-periodic.

This is the main idea behind the cut and project scheme. Starting from a higher-dimensional periodic lattice, you can obtain an aperiodic tiling by considering the projection of a ‘slice’ of that lattice onto the *physical space* of two or three dimensions. In our example above, we obtained a two-dimensional aperiodic tiling as a projection from a three-dimensional cubic lattice.

As it turns out, the Penrose and Ammann-Beenker tilings both can be described in this way. However, you need to employ four-dimensional lattices to do this. In four dimensions, it is possible to have symmetry axes of order 5 or 8 in a periodic lattice, and indeed the Penrose and Ammann-Beenker tilings are planar projections of appropriate ‘slices’ of the corresponding four-dimensional lattices, along the high-symmetry direction, such that the resulting tiling inherits the rotational symmetry.

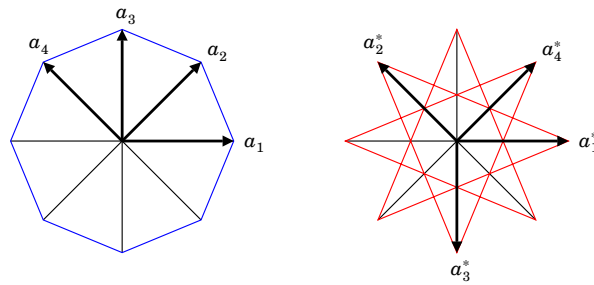


**Fig. 12.** The vectors  $a_k$ ,  $k = 1, \dots, 4$  spanning the  $\mathbb{Z}$ -module  $\Lambda$  in ‘physical’ space, and the corresponding vectors  $a_k^*$  spanning the ‘internal’ space.

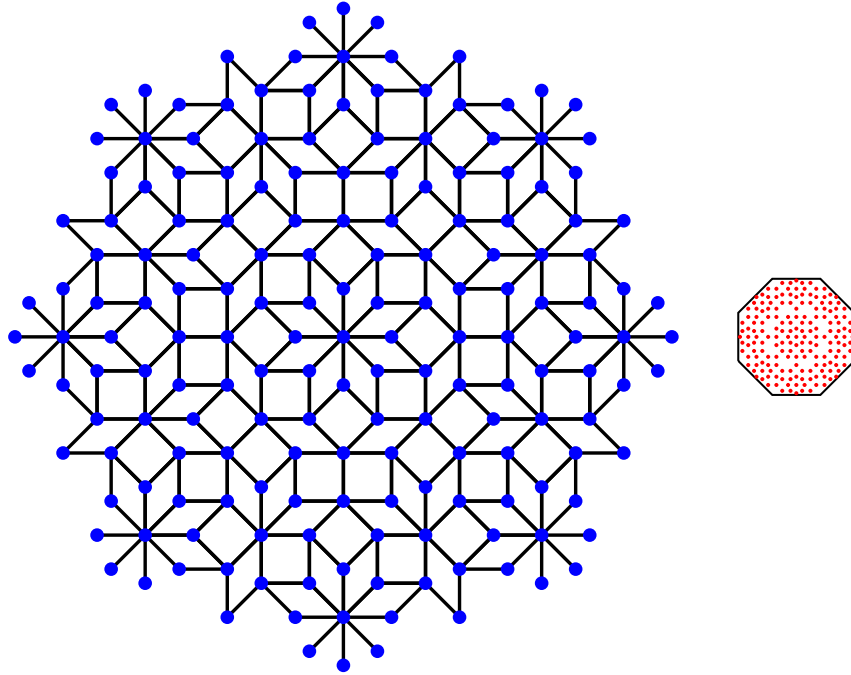


**Fig. 13.** The Ammann-Beenker tiling as a cut and project set. On the left, the projected points  $V_{AB}$  of the hypercubic lattice in physical space are shown, with lines connecting points of unit distance. On the right, the corresponding projections  $V_{AB}^*$  in internal space are shown, which fall into a regular octagon of unit edge length.

Explicitly, for the Ammann-Beenker tiling the cut and project approach can be implemented as follows. Consider the  $\mathbb{Z}$ -module of all integer linear combinations of the four vectors  $a_k$ ,  $k = 1, \dots, 4$ , shown in Fig. 12 on the left,

$$\Lambda = \{n_1 a_1 + n_2 a_2 + n_3 a_3 + n_4 a_4 \mid (n_1, n_2, n_3, n_4) \in \mathbb{Z}^4\}$$

which gives you a point set that is dense in the plane, corresponding to the projection of the entire hypercubic lattice  $\mathbb{Z}^4$  onto the ‘physical space’. From these, select all points for which the corresponding integer linear combination  $n_1 a_1^* + n_2 a_2^* + n_3 a_3^* + n_4 a_4^*$  of the vectors  $a_k^*$ , shown on the right in Fig. 12, falls into a regular octagon  $O$  of unit edge length. The vectors  $a_k^*$  span the projection of the hypercubic lattice  $\mathbb{Z}^4$  in the *internal space*. The octagon defines the ‘slice’ of the hypercubic lattice that is projected, and is called the *window* or *acceptance domain* of the cut and project scheme. Explicitly, the set of vertex points of the Ammann-Beenker tiling is given by

$$V_{AB} = \{x \in \Lambda \mid x^* \in O\},$$

and an example is shown in Fig. 13.

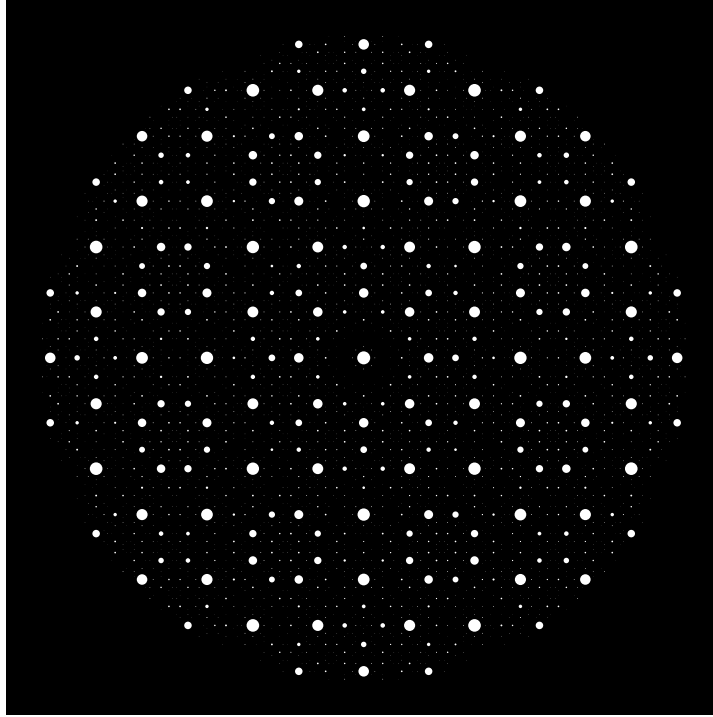


**Fig. 14.** Calculated diffraction image of the Ammann-Beenker tiling.

It can be shown that, under rather general assumptions, cut and project sets defined in this way possess a pure point diffraction measure. As an example, the calculated diffraction pattern of scatters positioned on the vertices of an Ammann-Beenker tiling is shown in Fig. 14.

## 2 Quasiperiodic functions, tilings and coverings

We proceed to a closer look at the mathematics. Periodic order as found in Euclidean space  $E^3$  is analysed in terms of a lattice  $\Lambda$ . Quasiperiodicity was viewed by H. Bohr on sections irrational with respect to a lattice  $\Lambda \in E^n$ . The study of quasicrystals showed how irrational sections emerge from forbidden point symmetry. The standard cell structure of periodic functions is absent in quasiperiodicity. The geometry of the lattice  $\Lambda \in E^n$  provides dual periodic Voronoi and Delone cell complexes. By the projection of boundaries from the dual complexes, a canonical tiling theory for quasiperiodic structures can be found and put in action.

## 2.1 Irrational subspaces and quasiperiodicity

We describe the geometry underlying H. Bohr's description [7] of quasiperiodicity.

Bohr (1925) considers an Euclidean space  $E^n$  with scalar product  $\langle, \rangle$  of dimension  $n$  and a periodic lattice  $\Lambda \in E^n$ . We first describe rational subspaces with respect to  $\Lambda \in E^n$ . Given the basis vectors  $(a_1, a_2, \dots, a_n)$  of  $\Lambda$ , the lattice points are determined by

$$\{t \mid t = \sum_j m_j a_j, (m_1, m_2, \dots, m_n) \in \mathbb{Z}^n\}. \quad (1)$$

The reciprocal lattice  $\Lambda^R$  has the basis  $(b_1, b_2, \dots, b_n)$ ,  $\langle b_i, a_j \rangle = \delta_{ij}$ . Any fixed reciprocal lattice vector  $b \in \Lambda^R$ , determines a rational hyperplane  $Y_b$  of the lattice  $\Lambda$  with points characterised by

$$Y_b = \{x \mid \langle x, b \rangle = 0\}. \quad (2)$$

This rational hyperplane is parallel to a hyperplane containing the lattice points

$$\{t \mid \langle t, b \rangle = 0\}. \quad (3)$$

A general rational linear subspace is the intersection of rational hyperplanes. Any other linear subspace for  $\Lambda \in E^n$  is called an irrational subspace with respect to  $\Lambda \in E^n$ .

*Example 1.* The irrational Fibonacci subspace of  $E^2$  is a line of slope  $\tau = \frac{1}{2}(1 + \sqrt{5})$  through the square lattice  $\Lambda = \mathbb{Z}^2$ . It is a horizontal line in Fig. 16. Below we shall construct the Fibonacci tiling on this irrational line.

A periodic function  $f^p(x)$ ,  $x \in E^n$  fulfils for all lattice translations  $t \in \Lambda$

$$f^p : f^p(x + t) = f^p(x). \quad (4)$$

Now split  $E^n$  into two orthogonal complementary linear subspaces

$$E = E_{\parallel} + E_{\perp}, \quad E_{\parallel} \perp E_{\perp}, \quad (5)$$

such that

- (i)  $E_{\parallel}$  is a subspace  $E_{\parallel} = E^m < E^n$  of dimension  $m < n$  and
- (ii)  $E_{\parallel}$  is irrational with respect to  $\Lambda \in E^n$ .

Define the Bohr class of quasiperiodic functions  $f^{qp}(x_{\parallel})$  as the restrictions of  $\Lambda$ -periodic functions  $f^p$  from  $E^n$  to  $E^m$ ,

$$f^{qp}(x_{\parallel}) := f^p(x)|_{x=x_{\parallel}+c_{\perp}}, \quad c_{\perp} = \text{const}. \quad (6)$$

Recall that the periodic function  $f^p$  has a pure point Fourier spectrum. By transferring the restriction of Eq. (6) to Fourier space, the quasiperiodic function  $f^{qp}$  can be shown to also possess a pure point spectrum. It is carried by a countable but dense module, compare Eq. (9) below. The Fourier analysis opens the way to the analysis of scattering from quasiperiodic structures in the same spirit as in ordinary crystallography.

## 2.2 Point symmetry

The non-crystallographic point symmetry found in quasicrystals produces irrational subspaces and quasiperiodicity of the Bohr class.

The discrete crystallographic point group  $G$  of a lattice  $\Lambda$  consists of orthogonal transformations  $D(G) < O(n)$  which carry  $\Lambda$  into itself. For given dimension  $n$ , all the space groups generated by pairs  $(\Lambda, D(G))$  are classified by the crystallography of  $E^n$  [8].

A point group  $G$  acting by  $D(G)$  on  $E^m$  but incompatible with any lattice  $\Lambda \in E^m$  is called non-crystallographic. Examples are the cyclic group  $G = C_5$  of order 5 in  $E^2$  and the icosahedral group  $G = H_3$  in  $E^3$ .

Mathematical schemes for aperiodic long-range order like the fivefold symmetric Penrose rhombus tiling [23] or the icosahedral rhombohedral tiling [16] displayed forbidden symmetries and preceded the experiments. The tacit assumption in physics until the year 1984 was that, since forbidden point symmetry was not compatible with any periodic lattice in  $E^3$ , there could be no long-range order with this point symmetry. The discovery of quasicrystals [25] in 1984 with icosahedral point symmetry disproved this assumption.

After 1984, non-crystallographic point symmetry turned out to play a key role for the understanding of new types of long-range order. The selection of a non-crystallographic point group generates the irrational subspace underlying the Bohr class of quasiperiodicity. To explain this we first claim that for any given group  $G$  of finite order  $|G| < \infty$  there exists a dimension  $n$  and a lattice embedding  $\Lambda \in E^n$  with point group a representation  $D(G) < O(n)$ . To show this we recall that, in the regular  $|G| \times |G|$  representation  $D^{\text{reg}}(G)$  of  $G$ , any element  $g \in G$  is represented by a permutation matrix. It then follows that the regular representation of  $G$  transforms the hypercubic lattice  $\mathbb{Z}^n$  into itself and so acts as a point group of this lattice. Of course it is technically desirable to look for the minimal lattice embedding of  $G$ . This can be achieved by the use of induced representations. In the next subsections we shall display minimal lattice embeddings.

Assume now that the  $n \times n$  representation  $D(G)$  admits a block diagonal reduction

$$D(G) \sim D'(G) \oplus D''(G), \quad (7)$$

where  $D'(G)$  acts non-crystallographically on  $E^m = E_{\parallel}$ . Then the decomposition, Eq. (5), of  $E^n$  meets the requirements for the Bohr class of quasiperiodic functions  $f^{ap}$ , and moreover these functions on  $E^m$  display the non-crystallographic point symmetry  $D'(G)$ .

*Example 2 (Fivefold point symmetry in  $E^2$  from the root lattice  $A_4 < E^4$ ).* The root lattice [3]  $A_4 < E^4$  has as point group a 4D representation  $D(S_5)$  of  $S_5$ , the symmetric group of order 5. The cyclic subgroup  $C_5 < S_5$  has two inequivalent real orthogonal 2D representations which for convenience we denote as  $D_{\parallel}(C_5)$ ,  $D_{\perp}(C_5)$ . In these two representations,  $C_5$  is generated by a rotation of angle  $2\pi/5$  and  $4\pi/5$ , respectively.

When the point group  $D(S_5)$  of  $A_4$  is restricted from  $S_5$  to  $C_5$ , one finds the block diagonal reduction

$$D(C_5) \sim D_{\parallel}(C_5) \oplus D_{\perp}(C_5). \quad (8)$$

But both 2D representations of  $C_5$  are non-crystallographic, and so the decomposition of Eq. (8) determines two orthogonal irrational planes in  $E^4$ . The plane  $E_{\parallel}$  is used for the Penrose and triangle quasiperiodic tilings discussed below.

On  $E^m = E_{\parallel}$ , the parallel projections of the lattice points of Eq. (1),

$$t_{\parallel} = \sum_j m_j (a_j)_{\parallel}, \quad (m_1, m_2, \dots, m_n) \in \mathbb{Z}^n, \quad (9)$$

form a  $\mathbb{Z}$ -module with basis the parallel projections of the lattice basis from  $E^n$  to  $E^m < E^n$ . In the Fourier analysis, it is shown that the Fourier amplitudes of a quasiperiodic function can be assigned to the reciprocal  $\mathbb{Z}$ -module spanned by the perpendicular projections to  $E_{\perp}$  of the reciprocal basis of  $A^R$ .

### 2.3 Dual Voronoi and Delone cell complexes and their projection

Dual Voronoi and Delone cell complexes in  $E^n$  provide periodic tilings of  $E^n$ . The Tübingen group of Kramer and coworkers since 1984 elaborated the significance of the dual cell complexes  $\mathcal{V}, \mathcal{D}$  for quasiperiodicity. The boundaries of the two complexes can be adapted to the irrational subspace  $E_{\parallel}$  and its orthogonal complement  $E_{\perp}$ . Parallel projections of boundaries provide tiles, perpendicular projections their coding windows.

The cell structure of crystals in  $E^n$  can, due to their periodicity, be encoded into cells modulo lattice translations. Clearly the values of a periodic function characterised by Eq. (4) can be fixed on a fundamental domain. In the language of group action, the fundamental domain is a set of points  $x \in E^n$  such that any other point of  $E^n$  can be reached from this set by a lattice vector from  $A$ . This fundamental domain may be taken as the unit cell, the parallelepiped spanned by the lattice vectors, or as the Voronoi domain  $V$ , defined below in Eq. (10).

The reasoning so far puts the structure analysis of quasicrystals into the frame of irrational embedding into a lattice and a space  $A \in E^n$ . Quasicrystals appear as crystallographic objects in  $E^n$ . Visualised in  $E^n$ , they represent quasiperiodic sections of dimension  $m$  through periodic objects in  $E^n$ . By definition of irrationality, the lattice vectors do not connect any two points on the subspace  $E^m$ . It follows that a cell structure for quasicrystals cannot be constructed modulo lattice translations. We now derive a canonical tiling structure by projection from dual boundaries of Voronoi and Delone cells of  $A \in E^n$ . The canonical projections from Voronoi and Delone complexes



were initiated in [16] and worked out for the fivefold symmetry in [3] and for icosahedral point symmetry in [17]. The general approach is given in [21, 18].

The Voronoi domain is an  $n$ -polytope around a lattice point  $t \in \Lambda$  defined as the set of points

$$V_t := \{x \in E^n : |x - t| \leq |x - t'| \text{ if } t' \neq t, t' \in \Lambda\}. \quad (10)$$

Any Voronoi domain has a hierarchy of boundaries  $X_p$  of dimension  $p$ ,  $0 \leq p \leq n$ , called  $p$ -boundaries. The Voronoi complex  $\mathcal{V}$  is the cell complex in  $E^n$  formed by the Voronoi domains of all lattice points. It fills  $E^n$ . Its  $p$ -boundaries form a hierarchy of subcomplexes of dimension  $p$ ,  $0 \leq p \leq n$ . A single fixed  $p$ -boundary  $X_p$  determines the set of all lattice vectors  $S_{X_p}$  whose Voronoi domains contain  $X_p$  as a boundary,

$$S_{X_p} := \{t \mid X_p \in V_t\}. \quad (11)$$

We define the  $(n - p)$ -polytope dual to  $X_p$  as the convex hull

$$X_{(n-p)}^* := \text{conv}(t \in S_{X_p}). \quad (12)$$

It can be shown that  $X_p$ ,  $X_{(n-p)}^*$  have indeed complementary dimension. The  $n$ -polytopes  $X_n^*$  are dual to the vertices  $X_0$  of the Voronoi domains and are called the Delone cells of the lattice  $\Lambda$ . They are centred at the vertices of the Voronoi domains, called the holes of the lattice. These vertices can be inequivalent under  $\Lambda$  and then give rise to inequivalent types of Delone cells. The Voronoi cells again fill  $E^n$  and form the dual Delone cell complex  $\mathcal{D}$  of  $\Lambda$ . The dual boundaries  $X_{(n-p)}^*$ ,  $0 \leq p \leq n$ , form the boundaries of the Delone cells. Both cell complexes for the root lattice  $A_2 \in E^2$  are illustrated in Fig. 15.

Given the dual boundary set from the Voronoi and Delone cell complex, we turn to the orthogonal decomposition of  $E^n$  given by Eq. (5). We introduce the projections of these boundaries to the parallel and perpendicular subspaces, denoted by the subindices  $\parallel, \perp$ . From pairs of parallel projections  $X_{m\parallel}$  and the orthogonal projections of their duals  $X_{(n-m)\perp}^*$  we form the set of the direct product polytopes

$$T = X_{m\parallel} \times X_{(n-m)\perp}^*. \quad (13)$$

These direct product polytopes turn out to be  $n$ -polytopes which provide a periodic tiling of  $E^n$ . By definition this periodic tiling has the particular property that all its tiles have their boundaries parallel or perpendicular to the subspace  $E^m$ .

Consider now a subspace  $E^m$  with fixed value of  $c_\perp$  according to Eq. (6). Its intersections with the tiling of  $E^n$  by the direct product polytopes  $T$ , Eq. (13), consists of shapes  $X_{m\parallel}$ , which form a finite variety of projected  $m$ -boundaries from the Voronoi complex  $\mathcal{V}$  or rather from its  $m$ -subcomplex  $\mathcal{V}^m$ . We call them the tiles of the quasiperiodic canonical tiling  $(\mathcal{T}, \Lambda)$  of  $E^m$ . The perpendicular projections in Eq. (13) are named the windows of the tiles.

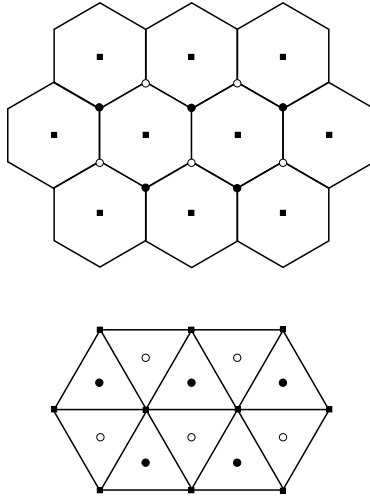


**Fig. 15.** Voronoi and dual Delone complex for the root lattice  $A_2$ . The Voronoi cells are hexagons centred at lattice points (black squares), the Delone cells triangles centred at two inequivalent types of holes (black and white cycles).

Windows can also be defined for vertices, for holes, and for covering clusters discussed below.

The dual Voronoi and Delone cell complexes allow for a second construction with the same subspaces but an alternative to Eq. (13). We interchange the role of the Voronoi and Delone complex, consider projected pairs of boundaries  $X_{m\parallel}^*$ ,  $X_{(n-m)\perp}$ , and form the direct product polytopes

$$T^* = X_{m\parallel}^* \times X_{(n-m)\perp}. \quad (14)$$

The intersection with  $E^m$  yields as tiles the projected  $m$ -boundaries of the Delone complex  $\mathcal{D}$ . This type of tiling we denote by  $(\mathcal{T}^*, \Lambda)$ . It is illustrated by the Fibonacci tiling in Fig. 16.

More examples for these quasiperiodic tilings will be given in the next subsections.

#### 2.4 Quasiperiodic functions compatible with a tiling

Once we have constructed a quasiperiodic tiling on the irrational subspace  $E^m < E^n$ , we return to a quasiperiodic functions  $f^{qp}$  of the Bohr class. By Eq. (6) these were given as the restrictions of  $\Lambda$ -periodic functions  $f^p$  to their values on the subspace  $E^m$ . This subspace, fixed by a perpendicular coordinate  $c_\perp$ , slices the periodic tiles  $T$  of Eq. (13) in varying vertical positions. Starting from a general  $\Lambda$ -periodic function  $f^p$  we cannot infer that  $f^{qp}$  obtained from it repeats its values on separate slices of a tile of fixed shape  $X_{m\perp}$ . In other words the functional values of a general quasiperiodic  $f^{qp}$  are still

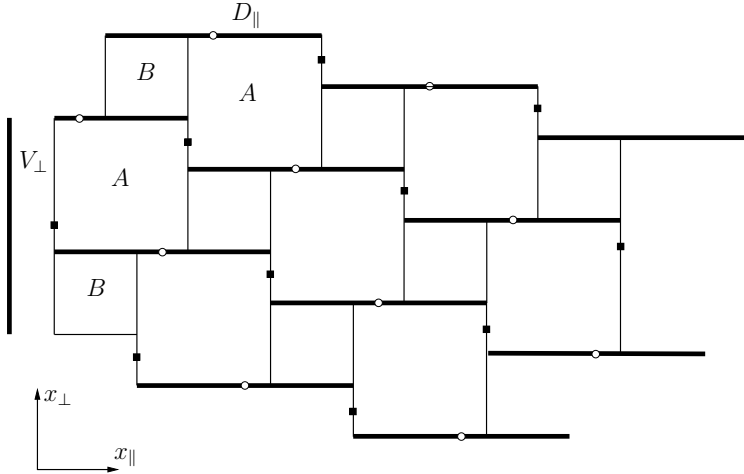


**Fig. 16.** Construction of the Fibonacci tiling. Two new squares  $A, B$  for  $\Lambda = \mathbb{Z}^2$  (lattice points black squares, holes white circles) play the role of the polytopes  $T^*$  in Eq. (14). The squares are constructed by projection from dual pairs of 1-boundaries and tile  $E^2$  periodically. The irrational horizontal Fibonacci line  $E_{\parallel}^1$  runs through this periodic tiling. Its intersections display the tiles  $A_{\parallel}, B_{\parallel}$  of the quasiperiodic Fibonacci tiling  $(\mathcal{T}^*, \mathbb{Z}^2)$ .

incompatible with the quasiperiodic tiling. Compatibility is achieved by the following construction:

Consider the periodic tiling of  $E^n$  by the polytopes  $T$  of Eq. (13). Restrict a  $\Lambda$ -periodic function  $f^p(x) = f^p(x_{\parallel} + x_{\perp})$  on any single polytope  $T$  to functional values independent of the coordinate  $x_{\perp}$ . Construct from this restricted  $f^p$  by Eq. (6) the corresponding quasiperiodic function  $f^{qp}$ . It follows that the functional values of  $f^{qp}$  are repeated on tiles of the same shape  $X_{m_{\parallel}}$ . The quasiperiodic function  $f^{qp}(x_{\parallel})$  is compatible with the tiling  $(\mathcal{T}, \Lambda)$ .

From compatible functions one can now construct the notion of a fundamental domain for quasiperiodic tilings [20, pp. 99–100]. As a consequence, the functional values of a compatible quasiperiodic function can now, as in crystals, be specified with reference to a bounded set of points on  $E^m$  modulo the projections of lattice translations. These concepts are put in action in the atomic structure and the physics of quasicrystals.

### 2.5 Quasiperiodic tilings from the lattices $A_4$ and $D_6$

We now illustrate the general constructions by examples. The root lattice  $A_4$  admits as its point group a 4D orthogonal representation  $D(S_5)$  of the symmetric group  $S_5$ . If we consider the cyclic subgroup  $C_5 \in S_5$ , the representation decomposes as given in Eq. (8) into two 2D representations. Each of them does not admit any periodic lattice in  $E^2$ . When we construct the

polytopes according to Eq. (13), we get a quasiperiodic tiling whose cells are projections of 2-boundaries of the Voronoi cells of  $A_4$ . These have two rhombus shapes and yield the tiling  $(\mathcal{T}, A_4)$  identical to the Penrose rhombus tiling shown in Fig. 17. Penrose [23] in 1974 constructed his rhombus tiling without use of any projection. De Bruijn [9] proved that it could be embedded into a 5D lattice. Our exposition follows the canonical minimal construction from the root lattice  $A_4 \in E^4$  given in [3].

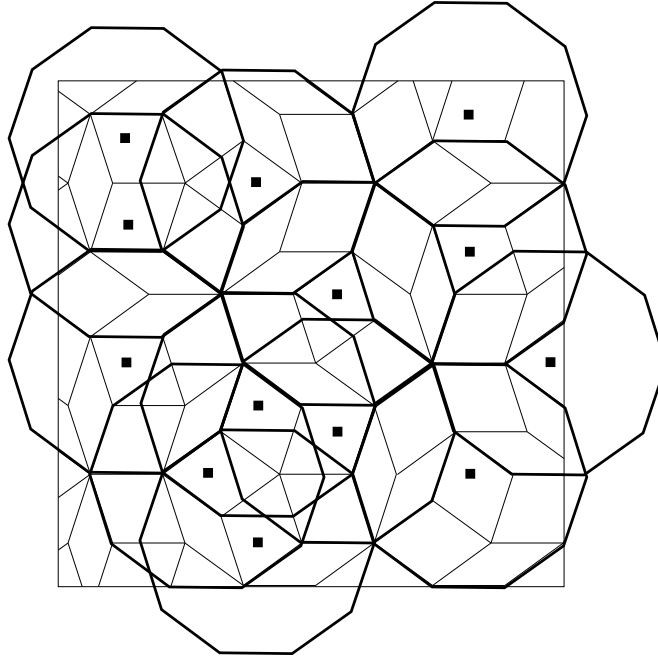


**Fig. 17.** The Penrose rhombus tiling  $(\mathcal{T}, A_4)$ . It consists of two types of rhombus tiles (thin lines), projections of 2-boundaries from the Voronoi complex. Any rhombus vertex is the projection of a hole from  $\Lambda = A_4$ . In addition we show a covering of the Penrose tiling by overlapping decagons (heavy lines) [13]. Each decagon covers 10 rhombus tiles and is centred at the projection of a lattice point (black square) of  $A_4$ .

If we use the alternative construction of Eq. (14), the tilings of the new tiling  $(\mathcal{T}^*, A_4)$  are projections of 2-boundaries of the Delone complex of  $A_4$ . These have two triangle shapes. The tiling is the Tübingen triangle tiling shown in Fig. 18.

In work published before the experimental finding, Kramer and Neri [16] in 1984 induced a 6D representation of the icosahedral group and embedded it minimally into the hypercubic lattice  $\mathbb{Z}^6$ . The corresponding quasiperiodic tiling  $(\mathcal{T}, \mathbb{Z}^6)$  with icosahedral point symmetry has two rhombohedral tiles,

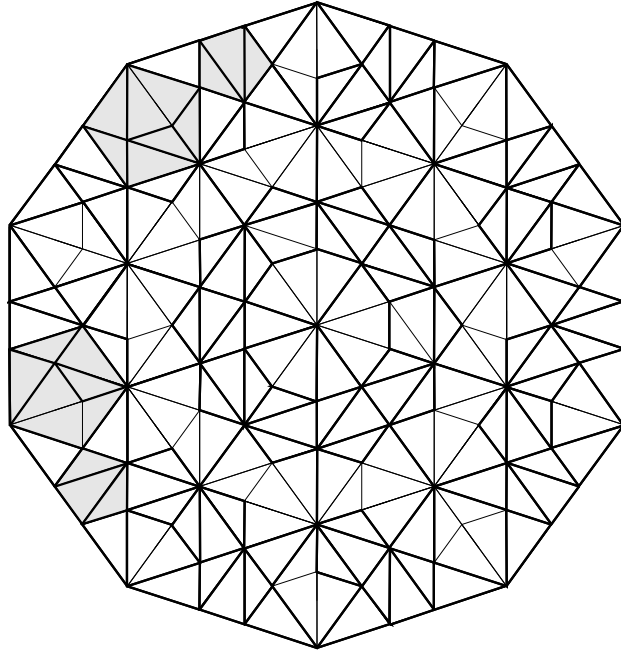


**Fig. 18.** The Tübingen triangle tiling  $(\mathcal{T}, A_4)$ . The tiles (thin lines) are two triangular projections of Delone 2-boundaries from the Delone complex. Any triangle vertex is the projection of a lattice point. In addition we show a covering of the triangular tiling by two types of overlapping pentagons (heavy lines).

compare Fig. 19. The root lattice  $D_6 \in E^6$  [17] admits the two dual constructions according to Eqs. (13) and (14), both with icosahedral point symmetry. These cases were worked out in detail and have been successfully applied to icosahedral quasicrystals.

In Fig. 19 we show the windows, compare Eq. (13) and what follows, and the tiles of the 3D Delone-based tiling  $(\mathcal{T}^*, D_6)$ . The lattice has three types of holes denoted by  $a, b, c$ . There are three corresponding types of Delone cells  $D^a, D^b, D^c$  whose perpendicular projections are shown in Fig. 19. The Delone 3-boundaries, and their projections which form the tiles, display as vertices these three types of holes.

## 2.6 Covering of quasiperiodic tilings

A new approach to quasiperiodic structure came with the idea of covering [13]. In a covering of a tiling, every tile becomes part of a small number of covering clusters. In contrast to a tiling, these clusters are allowed to overlap. Coverings of quasiperiodic structures are treated in detail in [20]. Here we give only two examples: The Penrose tiling  $(\mathcal{T}, A_4)$  is covered [19] by overlapping decagons,

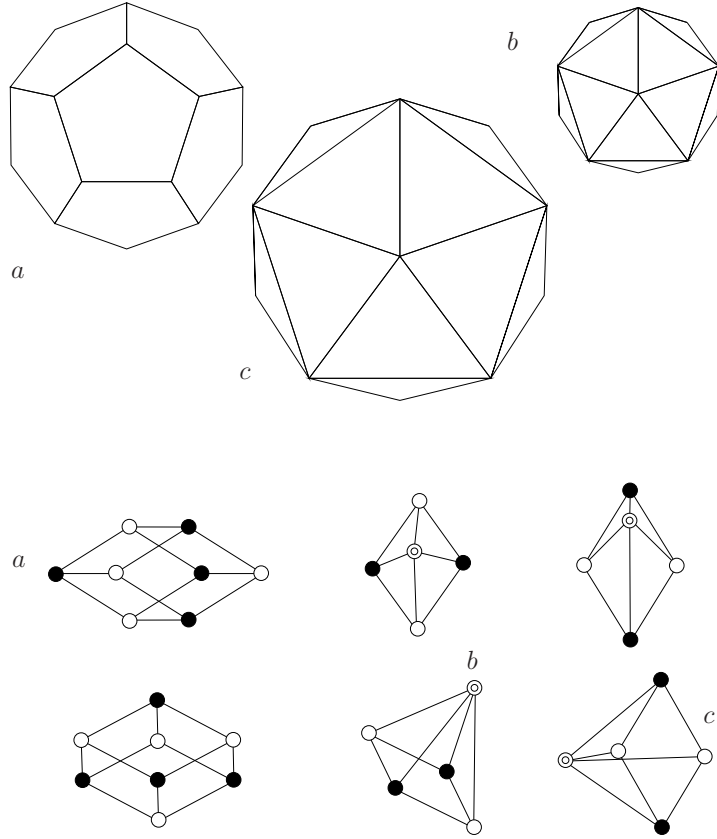


**Fig. 19.** The 3D icosahedral tiling  $(\mathcal{T}^*, D_6)$ . Top: The three Delone windows  $D_{\perp}^a, D_{\perp}^c, D_{\perp}^b \in E_{\perp}$  of the tiling  $(\mathcal{T}^*, D_6)$ . Bottom: The six tiles of this tiling are four pyramids on a rhombus base and the two rhombohedra known from the primitive tiling. The holes  $a, c$  are marked by black and white circles, the holes  $b$  by a double circle.

each consisting of 10 rhombus tiles. This covering is shown in Fig. 17. The triangle tiling  $(\mathcal{T}^*, A_4)$  is covered [19] by two types of pentagons as shown in Fig. 18.

*Acknowledgement.* UG acknowledges support by EPSRC via Grant EP/D058465. The authors thank D. Shechtman and P.C. Canfield, and the American Physical Society, for granting permission to reproduce Figs. 2 and 3 in this article.

## References

1. R. Ammann, B. Grünbaum, G.C. Shephard: Aperiodic tiles. *Discr. Comput. Geom.* **8**, 1–25 (1992)
2. M. Baake, U. Grimm, R.V. Moody: What is aperiodic order? arXiv: math.HO/0203252 (2002)
3. M. Baake, P. Kramer, M. Schlottmann, D. Zeidler: Planar patterns with five-fold symmetry as sections of periodic structures in 4-space. *Int. J. Mod. Phys. B* **4**, 21–25 (1988)
4. M. Baake and R. V. Moody (eds.): *Directions in Mathematical Quasicrystals*, CRM Monograph Series, vol. 13 (AMS, Providence, RI, 2000)
5. L. Bendersky: Quasicrystals with one-dimensional translational symmetry and a tenfold rotation axis. *Phys. Rev. Lett.* **55**, 1461–1463 (1985)
6. R. Berger: The undecidability of the domino problem. *Mem. Am. Math. Soc.* **66**, 1–72 (1966)
7. H. Bohr: Zur Theorie der fastperiodischen Funktionen. I: *Acta Math.* **45**, 29–127 (1925); II: *Acta Math.* **46**, 101–214 (1925)
8. R. Brown, R. Bülow, J. Neubüser, H. Wondratschek, H. Zassenhaus: *Crystallographic groups of four-dimensional space* (Wiley, New York 1978)
9. N.G. de Bruijn: Algebraic theory of Penrose’s non-periodic lattice. *Akad. Wetensch. Proc. Ser. A* **84**, 39–66 (1981)
10. I.R. Fisher, K.O. Cheon, A.F. Panchula, P.C. Canfield, M. Chernikov, H.R. Ott, K. Dennis: Magnetic and transport properties of single-grain  $R$ -Mg-Zn icosahedral quasicrystals [ $R = Y, (Y_{1-x}Gd_x), (Y_{1-x}Tb_x), Tb, Dy, Ho,$  and  $Er$ ]. *Phys. Rev. B* **59**, 308–321 (1999)
11. U. Grimm, D. Joseph: Modelling quasicrystal growth. In [26], pp. 199–218
12. U. Grimm, M. Schreiber: Aperiodic tilings on the computer. In [26], pp. 49–66
13. P. Gummelt: Penrose tilings as coverings of congruent decagons. *Geometriae Dedicata* **62**, 1–17 (1996)
14. T. Ishimasa, H.-U. Nissen, Y. Fukano: New ordered state between crystalline and amorphous in Ni-Cr particles. *Phys. Rev. Lett.* **55**, 511–513 (1985)
15. C. Janot: *Quasicrystals: A Primer*, 2nd ed. (Clarendon Press, Oxford, 1994)
16. P. Kramer, R. Neri: On periodic and non-periodic space fillings of  $E^n$  obtained by projection. *Acta Cryst. A* **40**, 580–587 (1984)
17. P. Kramer, Z. Papadopolos, D. Zeidler: Concepts of symmetry in quasicrystals: root lattice  $D_6$ , icosahedral group, etc. In: *Group Theory in Physics* ed. by A. Frank, T.H. Seligman, K.B. Wolf, AIP Conf. Proc. **266** (AIP, New York 1992) pp. 179–200
18. P. Kramer: Quasiperiodic Systems. In: *Encyclopedia of Mathematical Physics* ed. by J.-P. Francoise, G. Naber, Sh. Tsun Tsou (Elsevier, Oxford 2006) pp. 308–315
19. P. Kramer: Delone clusters, covering and linkage in the quasiperiodic triangle tiling. *J. Phys. A* **33**, 7885–7901 (2000)
20. P. Kramer, Z. Papadopolos (eds.): *Coverings of Discrete Quasiperiodic Sets, Theory and Applications to Quasicrystals* (Springer, Berlin 2003)
21. P. Kramer, M. Schlottmann: Dualization of Voronoi domains and klotz construction: a general method for the generation of proper space filling. *J. Phys. A* **22**, L1097–L1102 (1989)
22. R. V. Moody (ed.): *The Mathematics of Long-Range Aperiodic Order*, NATO ASI Series C 489 (Kluwer, Dordrecht, 1997)

23. R. Penrose: The role of aesthetics in pure and applied mathematical research. *Bull. Inst. Math. Appl.* **10**, 266–271 (1974)
24. M. Senechal: *Quasicrystals and Geometry* (Cambridge University Press, Cambridge, 1995)
25. D. Shechtman, I. Blech, D. Gratias, J.W. Cahn: Metallic phase with long-range orientational order and no translational symmetry. *Phys. Rev. Lett.* **53**, 1951–1953 (1984)
26. J.-B. Suck, M. Schreiber, P. Häussler (eds.): *Quasicrystals: An Introduction to Structure, Physical Properties, and Applications* (Springer, Berlin 2002)
27. H.-R. Trebin (ed.): *Quasicrystals* (Wiley-VCH, Weinheim, 2003)
28. M. Wang, H. Chen, K.H. Kuo: Two-dimensional quasicrystal with eightfold rotational symmetry, *Phys. Rev. Lett.* **59**, 1010–1013 (1987)